

PREDICTION OF INTERFACE RANDOM AND TRANSIENT ENVIRONMENTS  
THROUGH THE USE OF MECHANICAL IMPEDANCE CONCEPTS

Gary K. Jones and Frank J. On  
NASA, Goddard Space Flight Center  
Greenbelt, Maryland

Theoretically, the launch vehicle/spacecraft interface dynamics can be predicted through the use of mechanical impedance relations. The primary purpose of this investigation was to verify the practicality of this technique for the case of one-dimensional motion produced by (1) a random force input (bandlimited white noise) and (2) a transient force input (a half-sine pulse).

The required mechanical impedance relations were developed and the prediction technique computerized. The feasibility of the prediction technique was evaluated by comparing the interface predictions to the measured interface values obtained from laboratory tests of a one-dimensional model of a launch vehicle/spacecraft system.

For random input the prediction was made in terms of interface acceleration spectral density (PSD), while for the transient input the prediction was in terms of interface acceleration time history and its Fourier transform.

The results of this investigation indicated that the prediction technique gave satisfactory values for random force inputs but for the case of transient inputs it lacked sufficient accuracy. Thus, this investigation demonstrated that the mechanical impedance based prediction technique is practical for the prediction of interface environments due to random inputs for one-dimensional motions.

Although the prediction technique did not yield the desired accuracy in predicting the interface environment due to transient inputs, the investigation did define the reasons for the inaccuracies. The lack of accuracy in the prediction for the case of transient input was attributed to the manner in which impedance quantities were recorded and transferred to the computerized prediction scheme. Improvements are recommended in the data handling scheme to increase the accuracy of the transient predictions so as to make it a practical analysis tool.

N 71 - 76400

(ACCESSION NUMBER)

10

(PAGES)

TMX 67400  
(NASA CR OR TMX OR AD NUMBER)

(THRU)

(CODE)

(CATEGORY)

## INTRODUCTION

The development of spacecraft test specifications for random vibration and transient acceleration environments, which provide a good simulation of actual flight condition, has been of considerable interest to spacecraft designers. Normally the engineer makes use of flight data from previous flights of other spacecraft on the same basic launch vehicle to estimate in a statistical sense the levels of the random or transient inputs to the unflown spacecraft. The major assumption normally made in this approach is in assuming that the interface environment is unaffected by variations in the characteristic properties of the spacecraft structures so long as the spacecraft weights remain reasonably close.

It is also generally assumed that over a wide range of possible inputs to the spacecraft structure, the most severe condition to which the structures will be subjected is the envelope of the maxima of all possible inputs or some lesser value determined by use of statistical limit curves. Due to these assumptions, the test specifications so derived are unrealistic to an unknown degree. These test specifications may represent a severe overtest of the structure or conversely yield an unconservative test.

This investigation was directed toward predicting through the use of mechanical impedance concepts (References 1, 2 and 3) the interface environments of a one-dimensional model of a launch vehicle-spacecraft system resulting from (1) a random force input and (2) a transient force input. Note that the prediction of interface motion for the case of steady state sinusoidal input has been demonstrated (References 4 and 5). In this investigation (random/transient) and the Reference 4-5 investigation the input forces were applied to the launch vehicle end of the model. The feasibility of the prediction technique was determined by comparing the predicted environments to the actual measured environments.

## PREDICTION TECHNIQUE

A prediction technique based on mechanical impedance theory (Reference 1) was used to obtain the predicted values of interface power spectral density (due to random inputs) and interface acceleration time history and its Fourier transform (for the transient input). Consider two launch vehicle-spacecraft configurations, A and B, having the same launch vehicle, but

different spacecraft. If the interface driving point impedances or mobilities of both configurations are known, it is theoretically possible to determine a transfer relation between the configurations such that the interface PSD for configuration B can be predicted from the known PSD of configuration A. Similarly, the interface transient response for configuration B can be predicted from the known configuration A interface transient response.

Two physical test models (masses, springs and dampers) simulating launch vehicle-spacecraft systems were developed and were designated configurations A and B. Illustrated in Figure 1 is the configuration A and B test model. Math model representations of the test models were derived and are presented in Figure 2. The shaker's armature assembly was considered to be a part of the launch vehicle system in order to expedite the model testing. Comparing the math model to the test model, the reader will note that the shaker is represented in the math model by two masses, a damper and spring. The modeling of the shaker was accomplished through the use of the shaker's measured driving point impedance.

To theoretically derive the required prediction equations, first consider the prediction of the configuration B interface power spectral density,  $PSD_B$ . Through the use of the equations of interconnection defined in Reference 1 for one dimensional systems, the interface power spectral density of configuration A,  $PSD_A$ , due to a random force input applied to the L/V portion of the system can be expressed as:

$$PSD_A(\omega) = \left| \frac{Y_A(\omega)}{Y_{L/V}(\omega) + Y_A(\omega)} \right|^2 \cdot PSD_F(\omega) \quad (1)$$

Where  $PSD_F$ , the free power spectral density, represents the power spectral density at the interface of the L/V when that terminal is unrestrained.  $Y_{L/V}(\omega)$  and  $Y_A(\omega)$  are the interface

driving point mobilities for the configuration A spacecraft (S/C) and launch vehicle (L/V) respectively. Note that both these and subsequent mobility terms are of the form " $\ddot{X}/F$ " and thus are acceleration mobilities. In terms of the driving point impedances,  $Z_A(\omega)$  and  $Z_{L/V}(\omega)$ , equation (1) can be expressed as:

$$PSD_A(\omega) = \left| \frac{Z_{L/V}(\omega)}{Z_A(\omega) + Z_{L/V}(\omega)} \right|^2 \cdot PSD_F(\omega) \quad (2)$$

where  $Z_{L/V}(w) = \frac{1}{Y_{L/V}(w)}$  and

$$Z_A(w) = \frac{1}{Y_A(w)}$$

Similarly, for configuration B, we obtain:

$$PSD_B(w) = \left| \frac{Y_B(w)}{Y_B(w) + Y_{L/V}(w)} \right|^2 \cdot PSD_F(w) \quad (3)$$

where  $Y_B(w)$  is the interface driving point mobility of the configuration B spacecraft. The free power spectral densities,  $PSD_F$ , expressed in equations (1) and (3) are identical, inasmuch as the L/V portions of configurations A and B are identical and the forcing functions are the same for both configurations.

Equating the common factor,  $PSD_F$ , in equations (1) and (3) yields:

$$PSD_B(w) = PSD_A(w) \cdot \left| \frac{Y_B(w)}{Y_A(w)} \cdot \frac{Y_{L/V}(w) + Y_A(w)}{Y_{L/V}(w) + Y_B(w)} \right|^2 \quad (4)$$

Or in terms of impedance rather than mobility, equation (4) can be expressed as:

$$PSD_B(w) = PSD_A(w) \cdot \left| \frac{Z_{L/V}(w) + Z_A(w)}{Z_{L/V}(w) + Z_B(w)} \right|^2 \quad (5)$$

$$\text{Where } Z_B(w) = \frac{1}{Y_B(w)}$$

Going through a similar derivation to determine the prediction equation for the Fourier transform,  $H_B(w)$ , of the configuration B interface transient acceleration response yields:

$$H_B(w) = H_A(w) \cdot \frac{Z_{L/V}(w) + Z_A(w)}{Z_{L/V}(w) + Z_B(w)} \quad (6)$$

Where  $H_A(w)$  is the Fourier transform of the configuration A interface acceleration. Once  $H_B(w)$  is obtained, the inverse transform of  $H_B(w)$  can be made, yielding the predicted configuration B interface transient acceleration time history,  $h_B(t)$ .

i.e.,

$$h_B(t) = \frac{1}{\sqrt{2\pi}} \int_{-\infty}^{+\infty} H_B(w) e^{-iwt} dw \quad (7)$$

Equations (5), (6) and (7) were solved through the use of a digital computer program for  $PSD_B$ ,  $H_B(w)$ , and  $h_B(t)$ . The input parameters for equations (5) and (6) were measured quantities obtained from model tests. A digital computer program using the Fast Fourier Transform Technique was written and used to calculate  $H_A(w)$  and  $h_B(t)$ . Block diagrams which illustrate the use made of these equations (Equations (5), (6) and (7)) in this investigation are presented in Figures 3 and 4.

Comparison of the predicted values obtained from equations (5) and (7) to the values obtained from physical tests of configuration B was made in order to determine the practicality and assess the relative accuracy of the mechanical impedance based prediction technique.

#### DESCRIPTION OF TEST PROGRAM AND DATA REDUCTION

To facilitate the investigation, a one dimensional mechanical mass-spring-damper system was constructed so as to be able to simulate either of two launch vehicle-spacecraft systems (configurations A and B). The simulated launch vehicle portions of both configurations were identical, but the spacecraft portions were different. Photographs of configuration A and configuration B are presented in Figure 1.

The model's springs were designed so as to accept a visco-elastic damping material. Although not required for this investigation, a modal survey of configurations A and B were conducted with the results tabulated in Table 1.

Each test model was horizontally suspended in a triangular suspension frame - "A" frame structure (Figure 1) which had been specifically designed to isolate the test model from extraneous vibration. Note that the triangular suspension frame incorporated adjustable spring mounts which enabled the accurate alignment of the model masses to eliminate transverse motion when the model was being forced along its longitudinal axis.

Measurements of interface driving point acceleration mobilities were made in both test configurations. A Pyeling Type V.50Mkl vibration generator was used to supply the 10 - 20 lb. swept sinusoidal force at the interface terminal required for these measurements. An Endevco impedance head, Model 2110, was used in conjunction

with the Spectral Dynamics system (Figure 5) to measure the interface driving point mobilities. A block diagram of this test setup is shown in Figure 6. The resulting mobility plots are presented in Figures 9 through 14.

A Ling 227L shaker was used to generate both the random and transient inputs to the configurations A and B test models. Control of the shakers input was accomplished through the use of an Optimization Inc. Model PA250 A. C. Power amplifier in the current regulation - D. C. coupling mode to drive the shaker. The input current to the shaker was controlled by this system so as to be independent of the shaker's table loading. Block diagrams of the random and transient test setup are presented in Figures 7 and 8. The amplitude and frequency linearity of the force control over the frequency band (2 Hz - 2.5 KHz) was estimated to be  $\pm 1\%$ ; phase shift referenced to the armature current was estimated to be  $\pm 7$  degrees. The technique of calibrating the input force level in terms of input armature current consisted of multiplying the moving element mass of the Ling shaker, in the no table load condition, by the measured table acceleration and relating it to the measured input current. Note that the dynamic mass of the shaker's moving element was found to be constant ( $\pm 1$  db) from 0 to 2 KHz.

The types of input forces used in this investigation were: a single half sine pulse (2 ms, 55 lb. peak) and bandlimited (6 Hz - 2 KHz, 21 lb. rms) white noise. The interface acceleration response resulting from these transient and random inputs were measured by an Endevco Model 2219 accelerometer. Cross axis motion at various mass locations was monitored through the use of triaxial accelerometers, Endevco Model 2228B.

The PSD's (Figures 15 and 16) of the interface accelerations resulting from the white noise force input were obtained through the use of analog techniques. The Fourier transforms of the measured interface acceleration time histories (Figures 17 and 20) resulting from the half-sine input were obtained (Figures 18, 19, 22 and 24) through the use of a digital computer program.

#### PRESENTATION AND DISCUSSION OF RESULTS

The usefulness of the prediction technique was determined by comparing the predictions to the measured values.

A comparison of the predicted Configuration B interface PSD for the random input to the measured Configuration B interface PSD is presented in Figure 16. Evident in the figure is the good agreement between the predicted and measured value. Comparison of the measured configuration B interface acceleration time history (Figure 20) to the predicted configuration B interface acceleration time history (Figure 21) indicates poor agreement between the two time histories. That is, the prediction technique yielded inaccurate results when attempting to predict the acceleration time history due to a transient input. If the comparison is made on a Fourier transform basis rather than time history (see Figures 22, 23, 24 and 25) the agreement between measured and predicted appears to be somewhat better; however, this is of little importance since the time histories exhibit such a large disagreement.

The reason as to why the prediction technique yields better results for the case of random force input in comparison to transient force input cannot be exactly defined; however, in retrospect certain reasons for this fact seem evident.

The errors implicit in measuring the mobility quantities are propagated in both of the prediction schemes (i.e., random and transient prediction). The random prediction is made in terms of a real spectral quantity (PSD) while the transient prediction is expressed as a complex spectral quantity (a complex Fourier transform) and also as a time history (the inverse of the predicted Fourier transform).

If we were just concerned with comparisons of predicted spectral (PSD or Fourier transforms) values to measured values the transient prediction would not appear to be much worse than the random prediction. However in the transient prediction the important comparison is between the predicted time history and the measured time history; this comparison when made indicated poor agreement between the predicted and measured time histories.

It appears that the added complexity of the transient prediction is such as to place more stringent requirements on the accuracy of the mobility measurements. To illustrate an example of one such requirement, close inspection of the transient prediction equation reveals an incompatibility in frequency resolution among the elements of the equation. The Fourier transform

has a frequency resolution of 1.5 Hz while the mobility relations have a frequency resolution of 10 Hz. It would seem reasonable to expect an improvement in the transient prediction if the frequency resolutions of the mobility data were increased to be approximately the same as that of the Fourier transform. Note that for the random case all the elements of the prediction equation had approximately the same frequency resolution.

A worthwhile future task would be to improve the mobility measurement and data handling system so as to reduce the overall error in the system and thereby improve the accuracy of the prediction of interface transient environments. The improvements could take the form of direct digital recording on magnetic tape of the mobility information rather than analog recording using X-Y plotters. This system would avoid the problem of trying to read with high accuracy mobility data from X-Y plotter generated graphs for use in the prediction equation.

#### CONCLUSIONS

The two main conclusions resulting from this investigation are:

(1) The results of this study demonstrated the practicality of predicting the interface dynamics for a one-dimensional system excited by random force inputs.

(2) The results of this study revealed certain problems in the use of mechanical impedance based prediction techniques to predict interface time

histories due to transient inputs. It appears that these problems could be resolved through improvement in the mobility recording and data handling aspects of the investigation so as to improve the accuracy of the mobility information input into the computer program.

#### REFERENCES

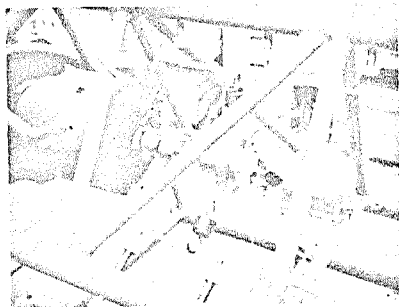
1. On, F. J., and Belsheim, R. O., "A Theoretical Basis for Mechanical Impedance Simulation in Shock and Vibration Testing of One-Dimensional Systems," NASA TN D-1954, August 1963.
2. On, F. J., "Mechanical Impedance Analysis for Lumped Parameter Multi-Degree of Freedom/Multi-Dimensional Systems," NASA TN D-3865, May 1967.
3. On, F. J., "Interconnection of Structural Systems by Use of Immitance Concepts," American Acoustical Society Meeting, Los Angeles, California, November 2-5, 1966.
4. On, F. J., and Jones, G. K., "Experimental Investigation of Interface Motion Prediction by Use of Mechanical Impedance Concepts - Steady State Sinusoidal Forces" Memo Report No. 681-14, July 5, 1968.
5. On, F. J., "A Verification of the Practicality of Predicting Interface Dynamical Environments by the Use of Impedance Concepts," The Shock and Vibration Bulletin, No. 38, Part 2, pp. 249-260, August 1968.

| Mode | Configuration A |                  | Configuration B |                  |
|------|-----------------|------------------|-----------------|------------------|
|      | Freq.<br>Hz     | c/c <sub>c</sub> | Freq.<br>Hz     | c/c <sub>c</sub> |
| 1    | 264             | .0086            | 229             | .0062            |
| 2    | 1081            | .0042            | 1090            | .0043            |
| 3    | 3892            | —                | 3962            | —                |

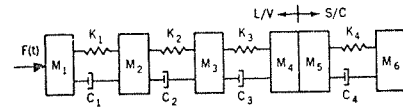
Modal Characteristics  
Launch Vehicle - Spacecraft Model  
Table 1



CONFIGURATION A TEST MODEL



CONFIGURATION B TEST MODEL



| LAUNCH VEHICLE L/V |                      |                         |                             |  |
|--------------------|----------------------|-------------------------|-----------------------------|--|
| i                  | M <sub>i</sub><br>lb | K <sub>i</sub><br>lb/in | C <sub>i</sub><br>lb-sec/in |  |
| 1                  | 1.02                 | 2.8 × 10 <sup>6</sup>   | 3.63                        |  |
| 2                  | 1.52                 | 20. × 10 <sup>6</sup>   | 248.                        |  |
| 3                  | 5.10                 | .86 × 10 <sup>6</sup>   | 1.40                        |  |
| 4                  | 21.25                | —                       | —                           |  |

| CONFIGURATION A<br>SPACECRAFT → S/C |                      |                         |                             | CONFIGURATION B<br>SPACECRAFT → S/C |                         |                             |
|-------------------------------------|----------------------|-------------------------|-----------------------------|-------------------------------------|-------------------------|-----------------------------|
| i                                   | M <sub>i</sub><br>lb | K <sub>i</sub><br>lb/in | C <sub>i</sub><br>lb-sec/in | M <sub>i</sub><br>lb                | K <sub>i</sub><br>lb/in | C <sub>i</sub><br>lb-sec/in |
| 4                                   | —                    | 0.8 × 10 <sup>5</sup>   | 0.40                        | —                                   | 0.95 × 10 <sup>5</sup>  | 0.42                        |
| 5                                   | 1.25                 | —                       | —                           | 1.25                                | —                       | —                           |
| 6                                   | 21.25                | —                       | —                           | 41.25                               | —                       | —                           |

Figure 2 Test Model Parameters

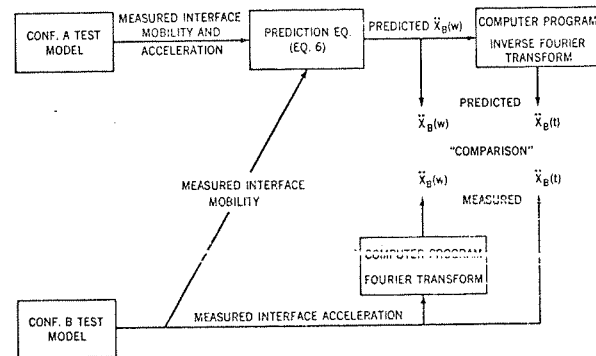


Figure 3 Investigation Block Diagram  
Random Input

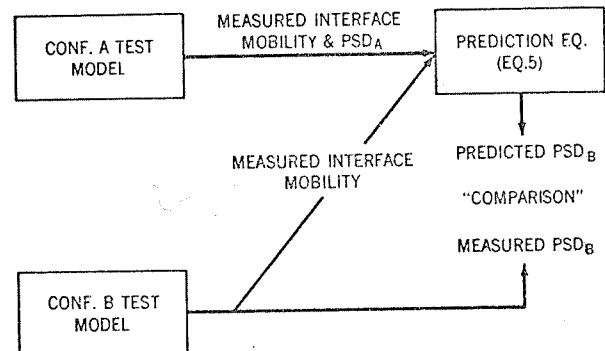


Figure 4 Investigation Block Diagram  
Transient Input

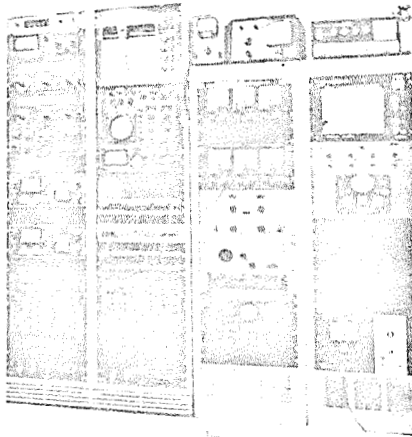


Figure 5 Automatic Impedance Analyzer System

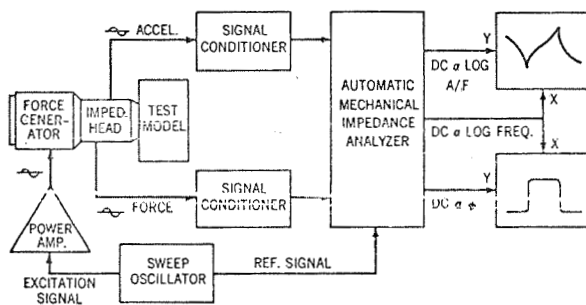


Figure 6 Block Diagram of Mobility Measurement Instrumentation

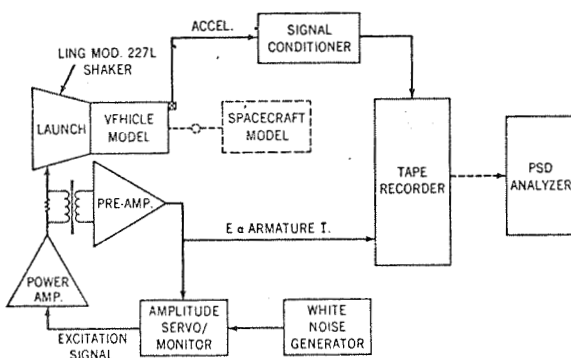


Figure 7 Block Diagram of Acceleration and Force Control Instrumentation - Random Input

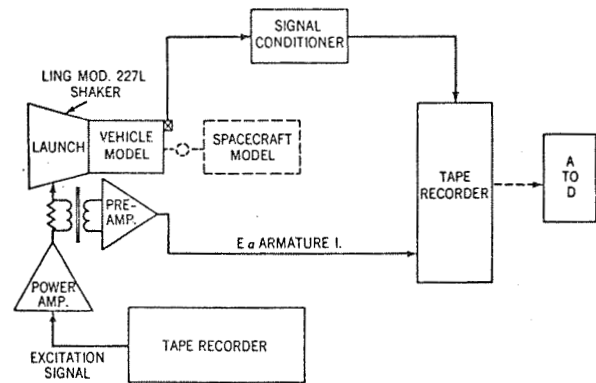


Figure 8 Block Diagram of Acceleration and Force Control Instrumentation - Transient Input

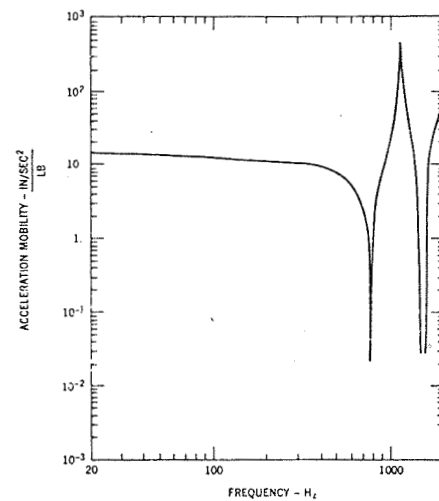


Figure 9 Interface Driving Point Mobility of L/V (Modulus)

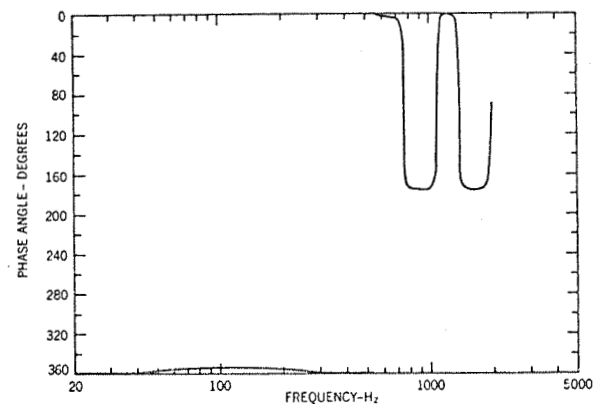


Figure 10 Interface Driving Point Mobility of L/V (Phase)

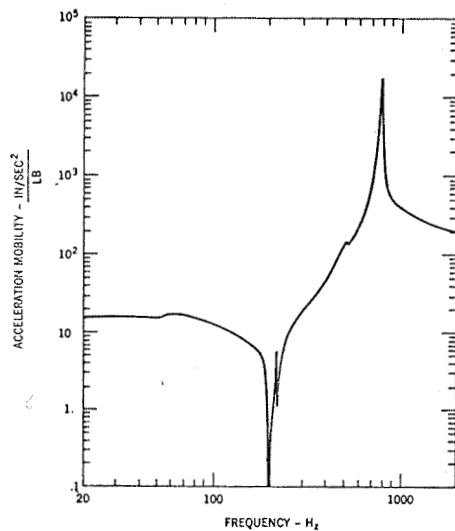


Figure 11 Interface Driving Point  
Mobility of Configuration A - S/C  
Model (Modulus)

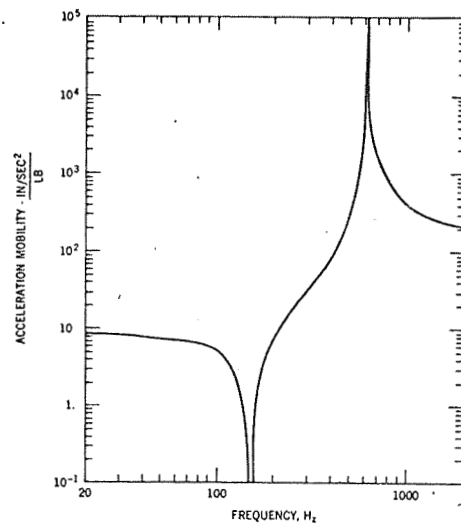


Figure 13 Interface Driving Point  
Mobility of Configuration B - S/C  
Model (Modulus)

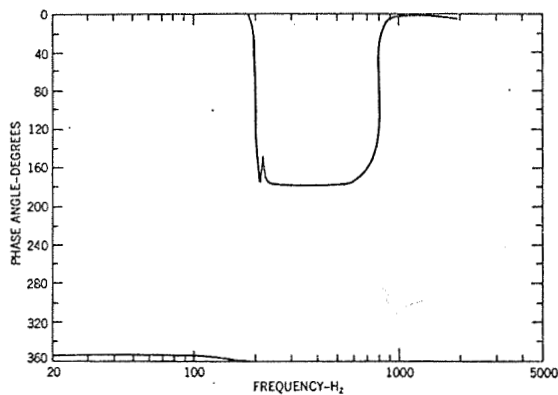


Figure 12 Interface Driving Point  
Mobility of Configuration A - S/C  
Model (Phase)

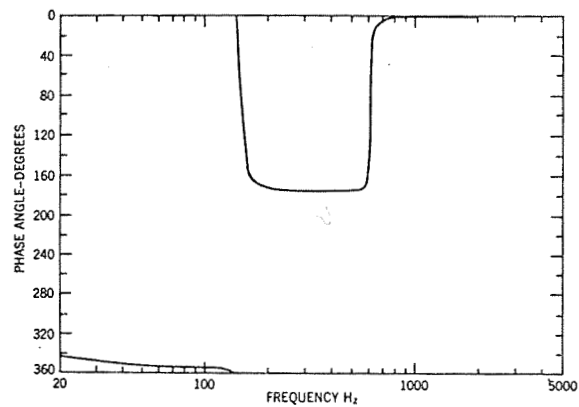


Figure 14 Interface Driving Point  
Mobility of Configuration B - S/C  
Model (Phase)

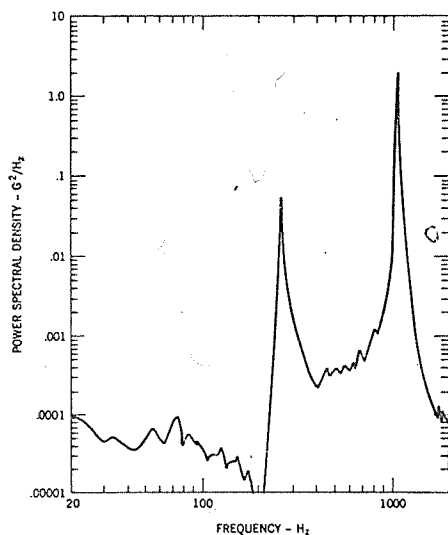


Figure 15 Power Spectral Density of Measured Configuration A Interface Acceleration (Random Input)

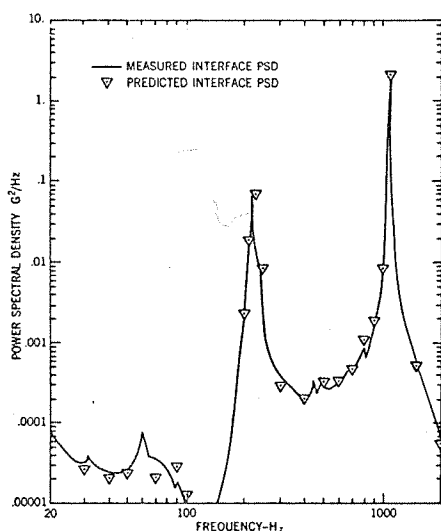


Figure 16 Measured Vs. Predicted Power Spectral Density of Configuration B Interface Acceleration (Random Input)

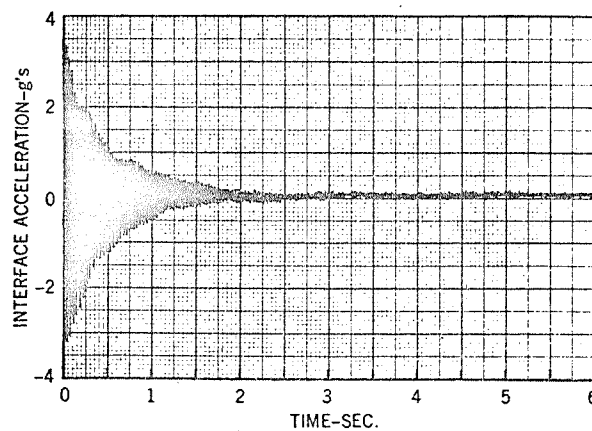


Figure 17 Measured Configuration A Interface Acceleration Time History (Transient Input)

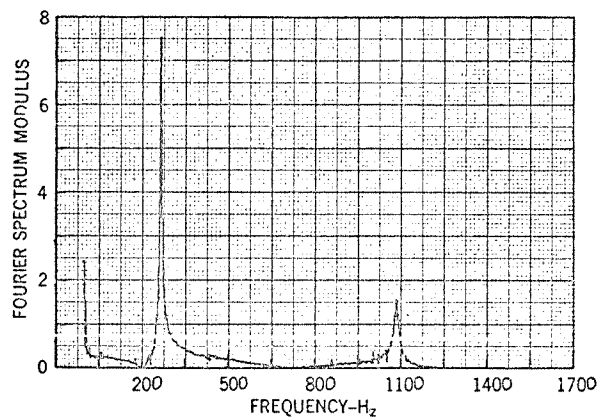


Figure 18 Fourier Transform of Configuration A Interface Acceleration Time History (Modulus)

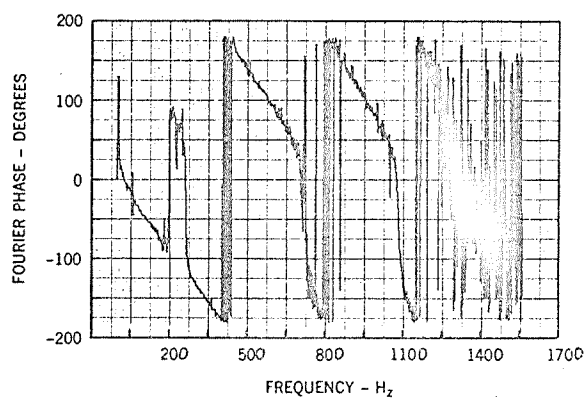


Figure 19 Fourier Transform of Configuration A Interface Acceleration Time History (Phase)

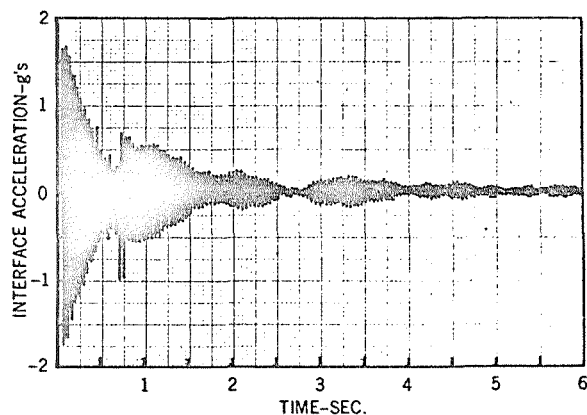


Figure 20 Measured Configuration B Interface Acceleration Time History (Transient Input)

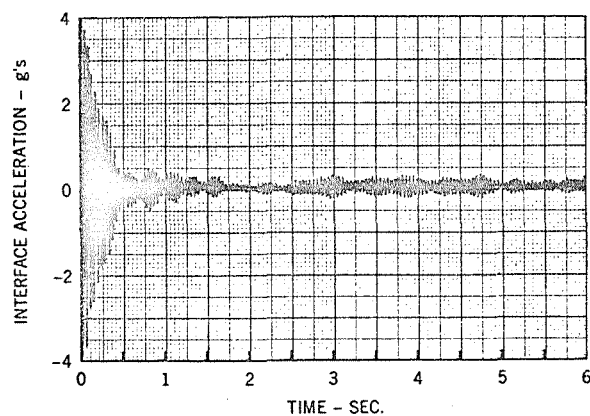


Figure 21 Predicted Configuration B Interface Acceleration Time History (Transient Input)

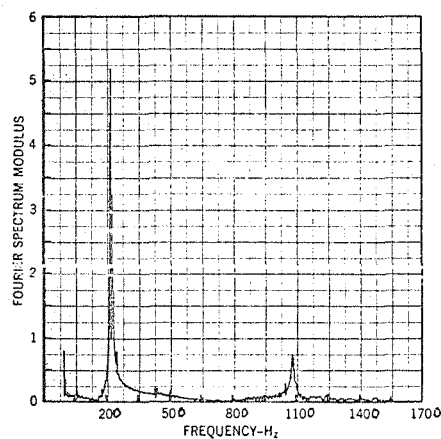


Figure 22 Fourier Transform of Measured Configuration B Interface Time History (Modulus)

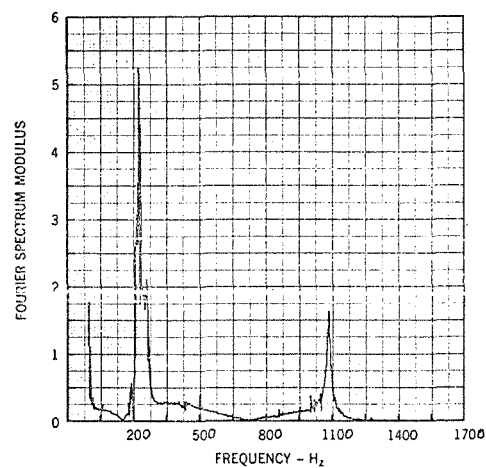


Figure 23 Fourier Transform of Predicted Configuration B Interface Time History (Modulus)

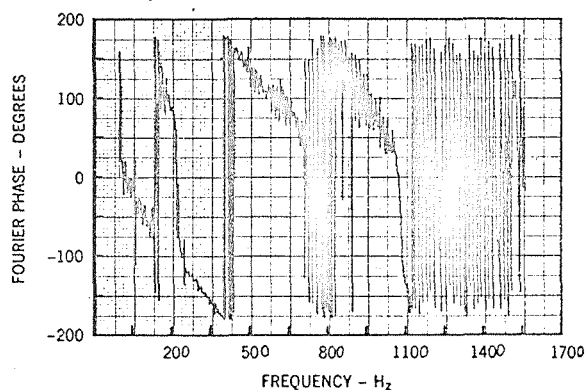


Figure 24 Fourier Transform of Measured Configuration B Interface Time History (Phase)

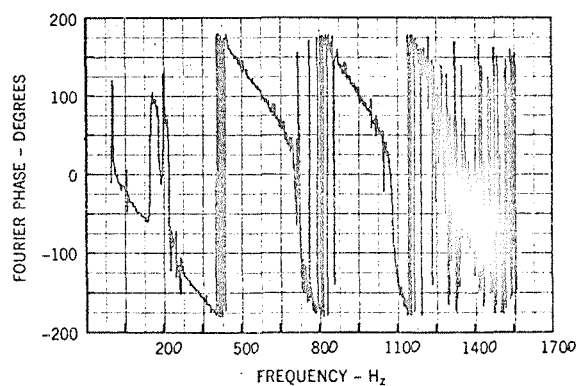


Figure 25 Fourier Transform of Predicted Configuration B Interface Time History (Phase)